Original Article

# Efficient Catalytic Synthesis of Xanthenes with Copper Immobilized on Amine-Modified NaY

**Mohammadreza Azizi Amiri** , **Hamidreza Younesi** , **Haniye Kazemi Aqmashhadi** , **Ghasem Firouzzadeh Pasha\*** , **Sakineh Asghari** , **Mahmood Tajbakhsh\***

*Department of Organic Chemistry, Faculty of Chemistry, University of Mazandaran, Babolsar 47416-95447, Iran*

## ARTICLE INFO

## ABSTRACT

The purpose of this article is to describe the synthesis of copper-amine complexes on nano NaY zeolite (Cu@NNPS-NaY), as a highly efficient, reusable, and environmentally friendly catalyst for the xanthenes synthesis. The Cu@NNPS-NaY catalyst was prepared from the reaction of silane-bonded nano NaY Zeolite (CPS-NaY) with [2-({3-[(2-aminoethyl) thio]propyl} thio)ethyl]amine (NN) followed by immobilizing copper ions onto the NNPS-NaY surface. The catalyst structure was characterized using FT-IR, XRD, TGA, EDS, DLS, SEM, TEM, ICP, and elemental analyses. The bonded long-chain amine including heteroatoms on the zeolite surface improved its catalytic activity and homogeneity, making it more capable of coordinating with copper ions. Synthesis of xanthenes was performed in the presence of Cu@NNPS-NaY catalyst (30 mg) in EtOH (10 mL) at 60 °C within 10-60 minutes resulting in product yields of 84-97%. The prepared catalyst can be easily recovered by centrifugation and reused for at least twelve consecutive runs with no significant loss of its catalytic activity. Besides the simplicity of catalyst recovery and reusing, the method is easy to set up and versatile, making it an environmentally friendly way to prepare titled heterocycles. Based on the results of this study, other useful heterocycles could be synthesized under eco-friendly conditions using this catalytic system.

\* Corresponding author: Mahmood Tajbakhsh and Ghasem Firouzzadeh Pasha
✉E-mail: tajbaksh@umz.ac.ir, ghasemf.pasha@umail.umz.ac.ir, ghasempasha@yahoo.com

**G R A P H I C A L A B S T R A C T**
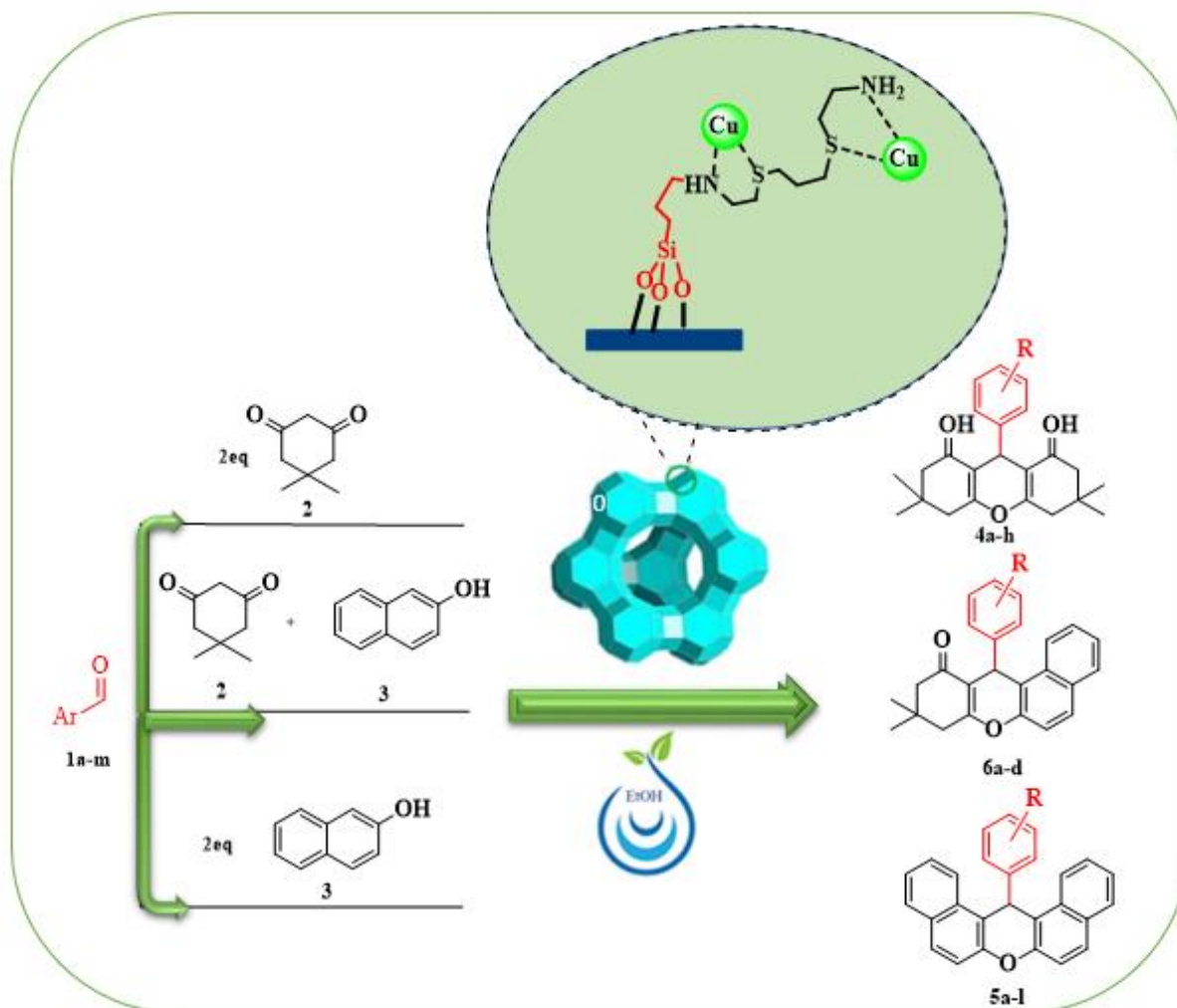


## Introduction

During the last few decades, catalytic processes have been associated with increasing health risks, and numerous efforts have been reported to reduce these risks [1,2]. Chemical reactions can be carried out using solid catalysts that are environmentally friendly and recyclable [3,4]. Among the most exciting research areas in chemistry is the homogenization of heterogeneous catalysts. Modification of heterogeneous catalysts increases catalytic reaction performance effectively. Nanomaterials have been used to immobilize a wide range of homogeneous catalysts to increase their reactivity, stability, and efficiency as catalytic agents [5,6]. The properties of nanozeolites, such as their availability, nontoxicity, reusability, high specific surface area, and nanoscale size, make them an effective nano-supporting substance [7]. There has been increasing interest in the zeolites

modification with organic molecules over the past few years [8]. As an example, amine-modified nanozeolites have been reported to act as heterogeneous catalysts, sorbents, and gas trappers in chemical reactions [9-11]. Organic compounds derived from xanthene are notable for their pharmacological and biological properties, which include antibacterial [12], antiviral [13], antitumor [14], antimalarial [15], and anti-inflammatory [16] properties. Furthermore, they can be used in pH-sensitive fluorescent materials [17], laser technology [18], and dyes [19]. Numerous catalytic methods reported for the synthesis of xanthenes using catalysts like Cu (II)-Fur-APTES/GO [20], $I_2$ [21], Cux-Cr100-x–MOF [22], Cobalt (II) complex [23], $NiCuFe_2O_4$ [24], $Fe_3O_4$@PS@His [$HSO_4^-$] [25], (TTTMS) [26], BioMOF-Mn [27], natural phosphate (NP) [28], [DMEA][$HSO_4$] [29], and Cu@CBA-Ze [11]. The use of heterogeneous catalysts in which organic components are

immobilized to porous solids offers significant advantages for synthetic processes such as selectivity and product removal. Our research aimed to present an impressive catalytic system for preparing heterocyclic compounds such as xanthenes [30,31]. It was demonstrated here that copper-amine complexes on nano NaY zeolite (Cu@NNPS-NaY) can be used as a nanocatalyst in the xanthenes synthesis (Scheme 1). To improve the catalytic activity and increase the capability of coordination with copper ions compound 2,2'-(propane-1,3-diylbis(sulfanediyl)) diethanamine (NN) including N and S heteroatoms immobilized on the silane-bonded nanozeolites surface (CPS-NaY). Because of the ease of recovery and reuse of catalyst, and the generality of the method as well as the use of EtOH as a solvent, this approach presents an environmentally friendly process for synthesizing titled heterocycles.

## Materials and Methods

From the Merck Company (Germany), the following chemicals were purchased: 3-chloropropyl trimethoxysilane (CPTMS), triethylamine, and solvents. Nano NaY zeolite (Si/Al =2.5) was prepared from the NaYlyst Corporation, USA. Ligand NN was prepared using a previously reported procedure [9]. The structure of synthesized products was identified by measuring their melting points (Thermal Electrothermal IA9100, Essex, UK), and acquiring their $^1$H- and $^{13}$C- NMR spectra (Bruker Avance DRX-400 spectrometer, Bruker, Germany). The structure of prepared samples was confirmed with various analyses such as FT-IR spectrometer (Bruker Tensor 27, Germany), scanning electron microscopy (SEM) (MIRA 3-XMU, Tescan, Brno, Czech Republic), dynamic light scattering (DLS) (HORIBA SZ-100, HORIBA, Japan), thermogravimetric analysis (TGA) (Netzsch, Selb, Germany), and X-ray powder diffraction (XRD) (Philips PW-1830, UK).

### Preparation of Copper-Amine Complexes on Nano NaY Zeolite (Cu@NNPS-NaY)

Under the $N_2$ atmosphere, 1 g of NaY Zeolite was heated in dry toluene (30 mL) for 30 minutes. To the mixture, 1.82 mL of CPTMS (10 mmol) was added and refluxed for 4 hours. The white powder (CPS-NaY) was centrifuged after cooling to room temperature. To purify and remove surface-absorbed CPTMS, a soxhlet extractor was used with ethanol [9]. For 30 minutes, the solution of 1 g of CPS-NaY in dry $CH_2Cl_2$ (30 mL) was stirred at room temperature under an $N_2$
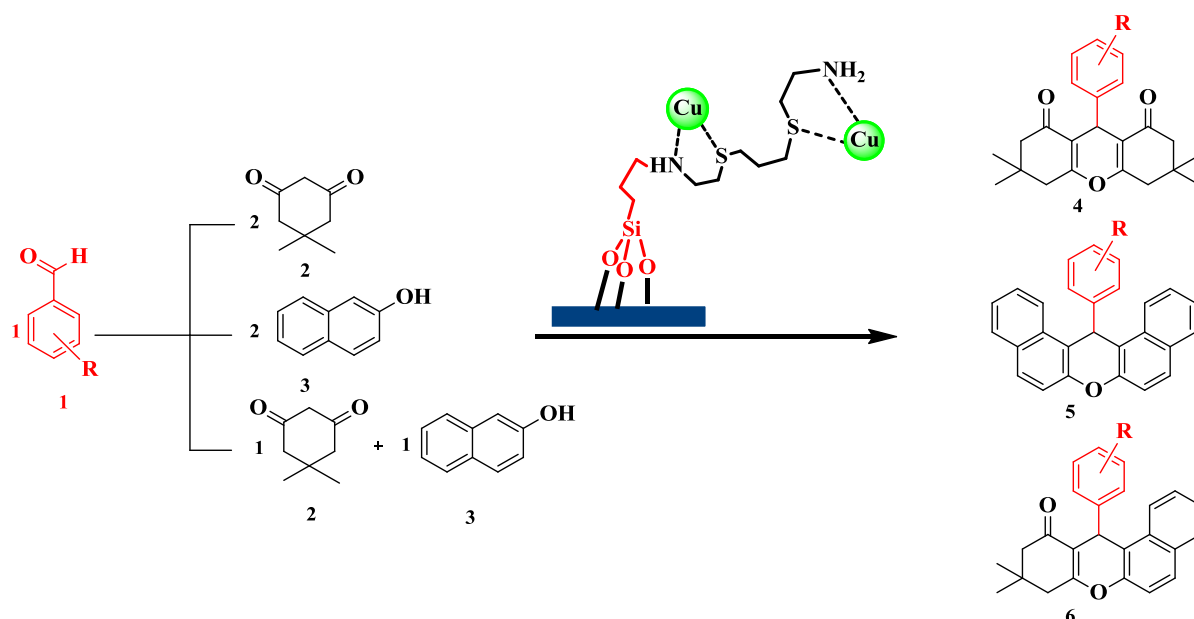


**Scheme 1:** Synthesis of xanthenes catalyzed by Cu@NNPS-NaY

atmosphere, and then 1.38 mL of triethylamine (10 mmol), and 1.94 g of compound NN (10 mmol) were added to the mixture and allowed to be stirred for 24 hours at ambient temperature. After centrifuging, amine-modified nanozeolite (NNPS-NaY) was collected and dried in a vacuum. To remove the unreacted NN, the NNPS-NaY was purified using a soxhlet extractor with ethanol [9]. To the mixture of 25 mL of CuI (1 M) was added 1 g of NNPS-NaY and stirred at 60 °C for 15 hours. After centrifugation, the Cu@NNPS-NaY was washed with deionized water. Scheme 2 displays a diagram illustrating the synthetic pathway.

### Synthesis of Xanthene Derivatives *4-6*

To a solution of aromatic aldehyde (1 mmol), dimedone (2 mmol) and/or *β*-naphthol (2 mmol) in 10 mL EtOH was added 30 mg Cu@NNPS-NaY catalyst and stirred at 60 °C for 30 minutes. TLC was used to check the reaction completion (EtOAc:n-hexane (3:1) as eluent), and then centrifugation was used to separate the catalyst. After removing the solvent under reduced pressure, the precepted product was recrystallized from ethanol. Copies of $^1$H- and $^{13}$C-NMR spectra of selected products **4-6** are contained in the supporting information.

### Spectral Data for Product *4a*

White powder, $^1$H-NMR (CDCl$_3$, 400 MHz): $\delta$ 1.01 (s, 6H, 2CH$_3$), 1.12 (s, 6H, 2CH$_3$), 2.19 and 2.25 (ABq, 4H, $J$ = 16.00 Hz, 2CH$_2$), 2.48 (s, 4H, 2CH$_2$), 4.77 (s, 1H, CH), 7.10 – 7.14 (m, 1H, CH$_{Ar}$), and 7.23 (t, 2H, $J$=8 Hz, CH$_{Ar}$), 7.30 – 7.32 (m, 2H, CH$_{Ar}$). $^{13}$C-NMR (CDCl$_3$, 100 MHz): $\delta$ 27.3, 29.2, 31.8, 32.2, 40.8, 50.7, 115.6, 126.3, 128.0, 128.3, 144.0, 162.2, and 196.3.

## Results and Discussion

The homogenized nano NaY zeolite was synthesized by post-modification of NaY zeolite with CPTMS and NN followed by coordination with Copper (I) ion. It is assumed that the dispersion of nanozeolite in the reaction solution is reduced, which could be due to the presence of hydroxyl groups on the nanozeolite surface. However, modification of nanozeolite using ligand NN enhances the dispersibility, and reactivity properties of nanozeolite. In addition, the presence of sulfur and nitrogen heteroatoms in the structure of the ligand NN increases the chelating ability of the nanozeolite. Copper-amine complex supported on nanozeolite (Cu@NNPS-NaY) was prepared by reacting NaY with CPTMS to afford silane-attached nanozeolite (CPS-NaY). The amine-modified NNPS-NaY was produced by reacting CPS-NaY with ligand NN followed by coordination with CuI to obtain copper amine-decorated nanozeolite (Cu@NNPS-NaY). The structure of all synthesized catalysts was identified by various analyses such as FT-IR, TGA, DLS, SEM, EDS mapping, XRD, TEM, ICP, and elemental analyses (Scheme 2).

In Figure 1, the FT-IR spectra of all catalysts and ligand NN are shown. The FT-IR spectra of NaY, CPS-NaY, NNPS-NaY, and Cu@NNPS-NaY exhibit distinct vibrational bands related to O-H stretching, O-H bending, and Si–O stretching at around 3500-3300 cm$^{-1}$, 1640 cm$^{-1}$, and 1060-1000 cm$^{-1}$, respectively. In the spectrum of CPS-NaY, the appearance of C-H stretching vibrations at around 2920-2960 cm$^{-1}$ confirms the successful bonding of CPTMS onto the NaY. The FT-IR spectrum of NN shows the vibrational signals at around 3350 cm$^{-1}$, 2952 cm$^{-1}$, and 1643 and 1459 cm$^{-1}$ ascribed to N–H vibrations, C–H vibrations, and NH$_2$ bending vibrations, respectively. In the FT-IR spectrum of NNPS-NaY, specific absorption bands are observed at frequencies 3376 cm$^{-1}$, 2933 cm$^{-1}$, 1641 cm$^{-1}$, and 1100 cm$^{-1}$ related to N–H vibrations, C–H vibrations, NH$_2$ bending, and Si–O–Si vibrations, respectively. This confirms the successful bonding of NN to the CPS-NaY surface. In the FT-IR spectrum of Cu@NNPS-NaY, all expected absorption bands similar to NNPS-NaY's FT-IR spectrum are observed with slight shifts [9-11].
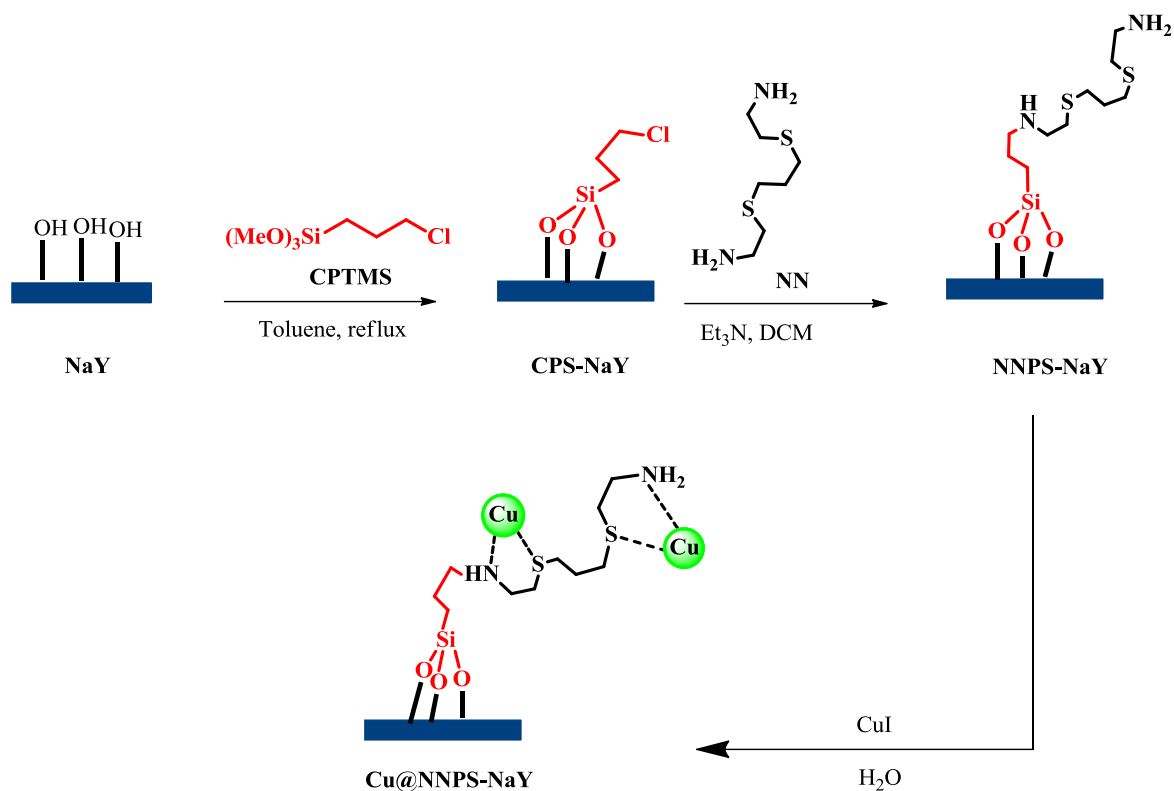
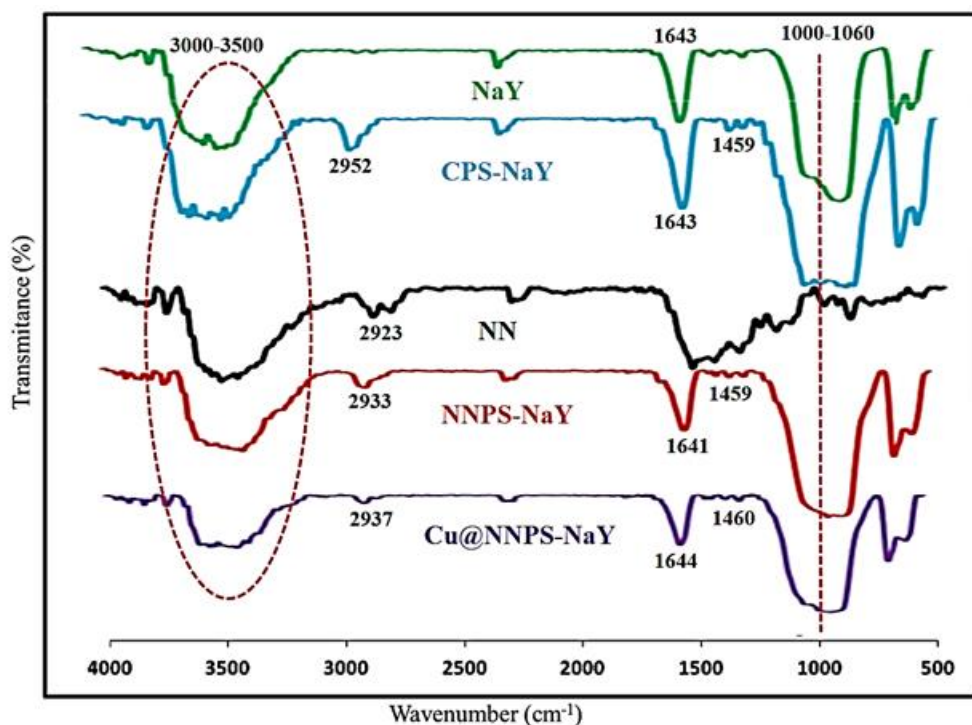**Scheme 2:** Preparation of the catalyst Cu@NNPS-NaY



**Figure 1:** FT-IR of NaY, CPS-NaY, NN, NNPS-NaY, and Cu@NNPS-NaY

The TGA curves of NaY, CPS-NaY, NNPS-NaY, and Cu@NNPS-NaY are depicted in Figure 2. The TGA of all samples shows a weight loss under 200 °C related to the physically adsorbed surface water. Also, the CPS-NaY, NNPS-NaY, and Cu@NNPS-NaY exhibit other weight loss between 200-400

°C corresponding to the removal of organic molecules. As can be seen, the thermal stability was decreased from NaY toward NNPS-NaY which confirming the modification of the NaY surface with CPTMS (2.07 mmol/g) and NN (1.23 mmol/g), respectively. Although the Cu@NNPS-NaY shows higher thermal stability due to copper immobilizing onto the NNPS-NaY's surface.

The determination of bonded-organic molecules onto the NaY surface was investigated by CHN analysis (Table 1). An increase in the carbon percentage and observation of nitrogen and sulfur atoms in the NNPS-NaY structure indicated that ligand NN was successfully bonded on the CPS-NaY surface. Based on nitrogen percentage, about 1.31 mmol/g ligand NN was attached to the CPS-NaY surface, which is in good agreement with TGA data. In addition, the amount of copper on the NNPS-NaY surface was analyzed using ICP and found to be 2.05 mmol/g.
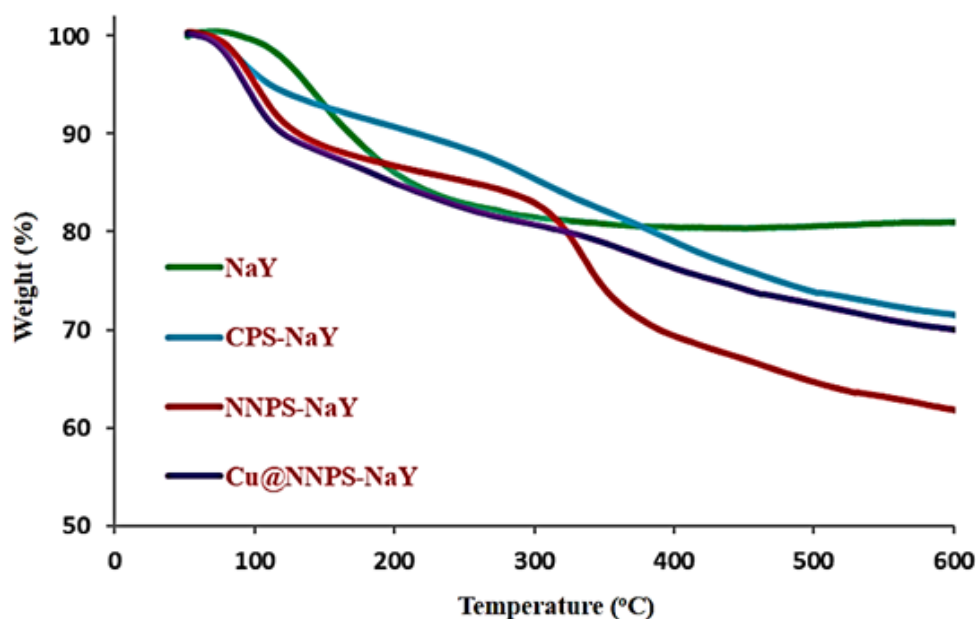


**Figure 2:** TGA thermograms of NaY, CPS-NaY, NNPS-NaY, and Cu@NNPS-NaY

**Table 1:** Results of the CHN analysis for CPS-NaY and NNPS-NaY

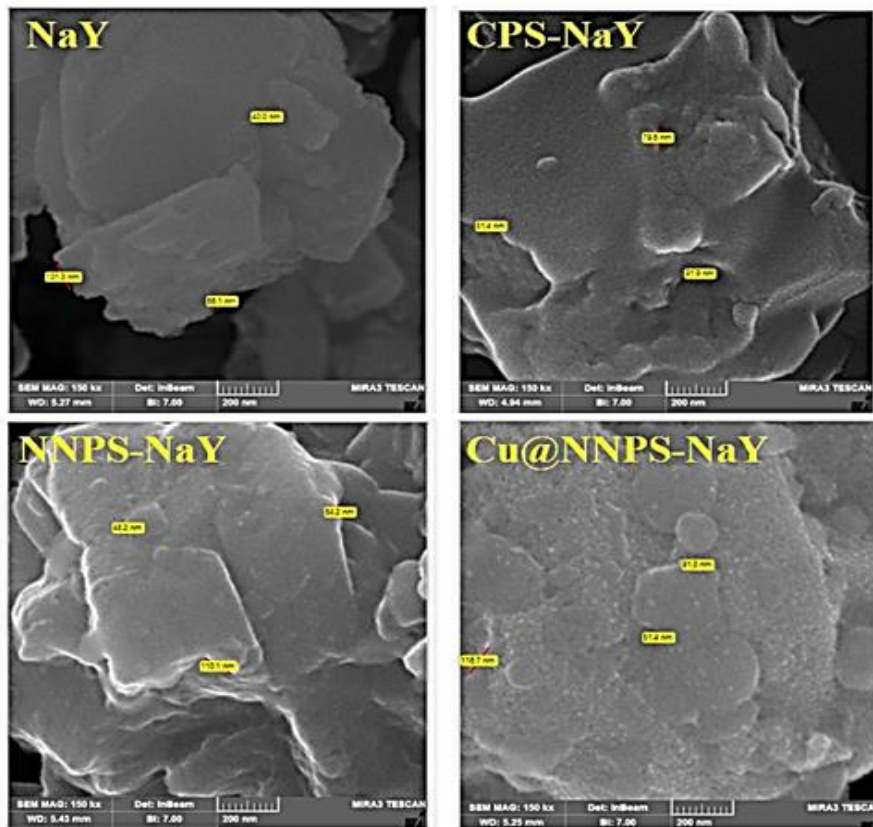| Entry | Catalyst | C (wt %) | N (wt %) | S (wt %) |
|-------|----------|----------|----------|----------|
| 1 | CPS-NaY | 7.84 | - | - |
| 2 | NNPS-NaY | 15.76 | 3.67 | 8.51 |

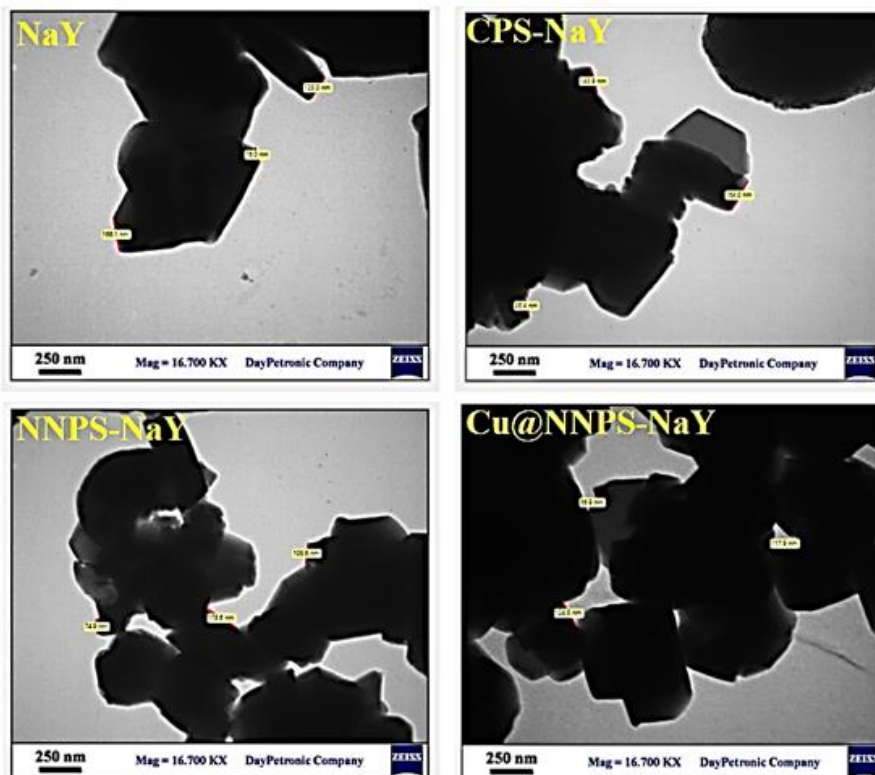**Figure 3:** SEM images of NaY, CPS-NaY, NNPS-NaY, and Cu@NNPS-NaY



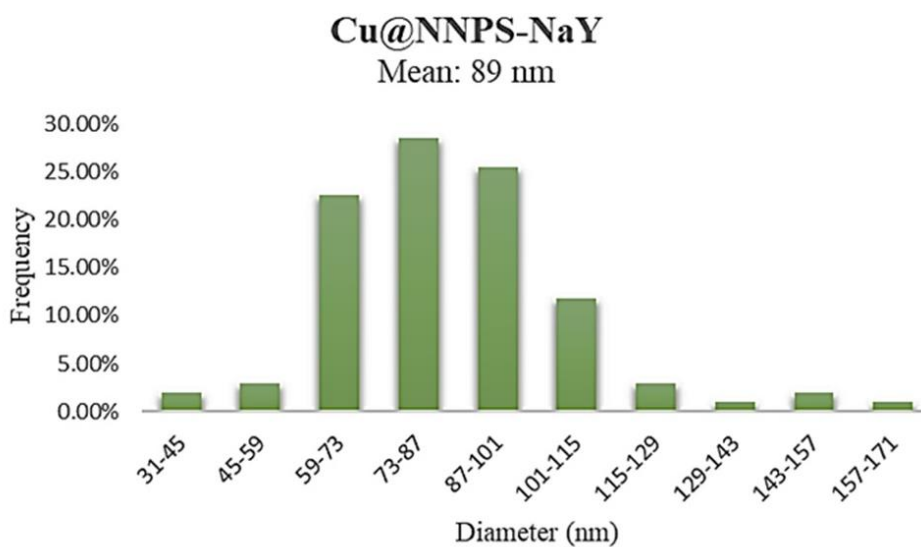**Figure 4:** The TEM image of NaY, CPS-NaY, NNPS-NaY, and Cu@NNPS-NaY

**Figure 5:** Size histogram patterns of Cu@NNPS-NaY

Figure 5 shows the particle size distribution histogram of Cu@NNPS-NaY, indicating an average particle size of 89 nm, which is slightly different than the results obtained with SEM.

As shown in Figure 6, the uniform distribution of Si, Al, O, N, C, and Cu in the elemental mapping analysis of the Cu@NNPS-NaY catalyst represents a uniform catalyst surface modification.
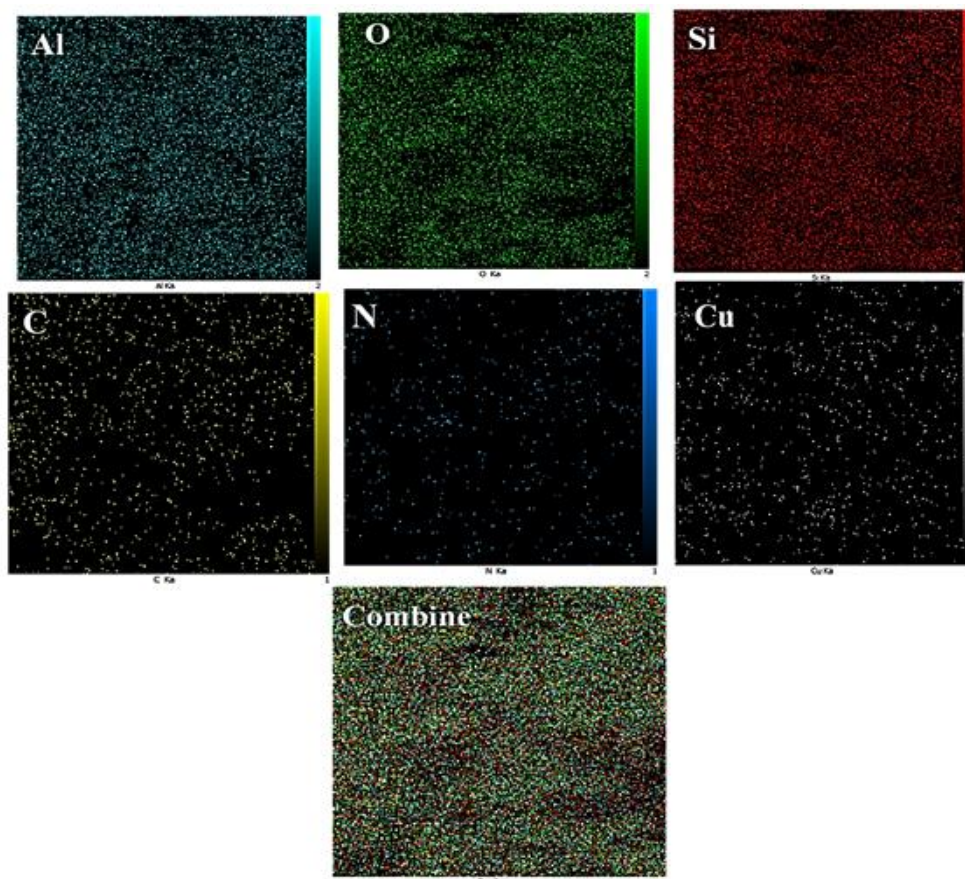


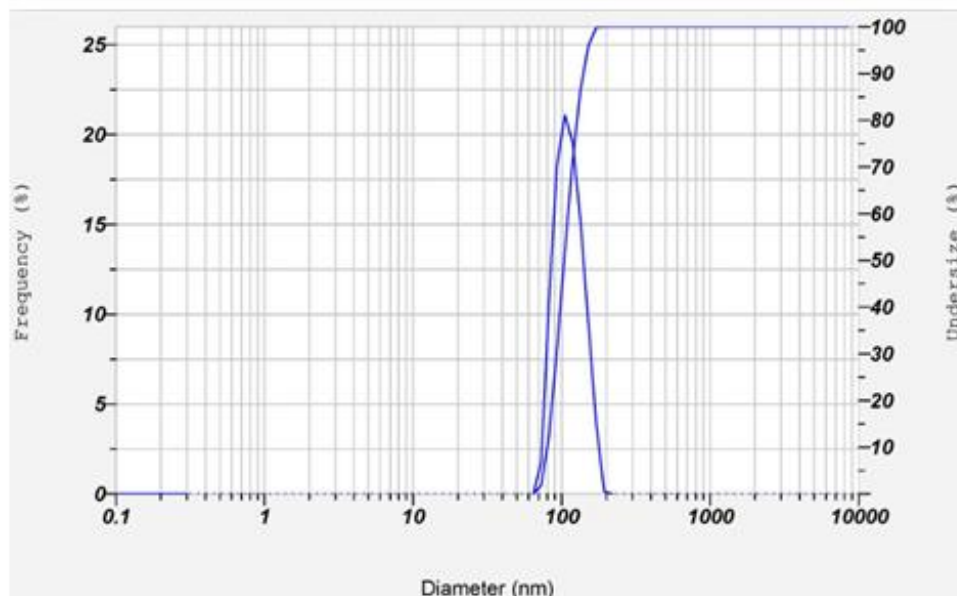**Figure 6:** Elemental mapping of the Cu@NNPS-NaY catalyst

**Figure 7:** DLS diagram of the Cu@NNPS-NaY

As depicted in Figure 7, the particle size distribution in the liquid phase of the Cu@NNPS-NaY was investigated by DLS analysis. The sample has a relatively uniform distribution of particle sizes, with an average particle size of 114 nm.

The X-ray diffraction patterns were applied to investigate the crystal structures of all NaY-based catalysts. In the 2θ=5-80, the XRD patterns of the NaY, CPS-NaY, NNPS-NaY, and Cu@NNPS-NaY exhibit all distinct NaY Zeolite reflection peaks confirming no significant changes were observed within the modification process of nano NaY Zeolite surface (Figure 8). Observation of two peaks at 2θ: 36.51° and 42.52° which corresponds to the $Cu_2O$ phase, exhibiting the successful supporting of copper ions onto the NNPS-NaY's surface [32-34]. Crystal sizes for NaY, CPS-NaY, NNPS-NaY, and Cu@NNPS-NaY were determined using the Debye-Scherrer equation: 19.15, 24.66, 24.65, and 18.47 nm, respectively.
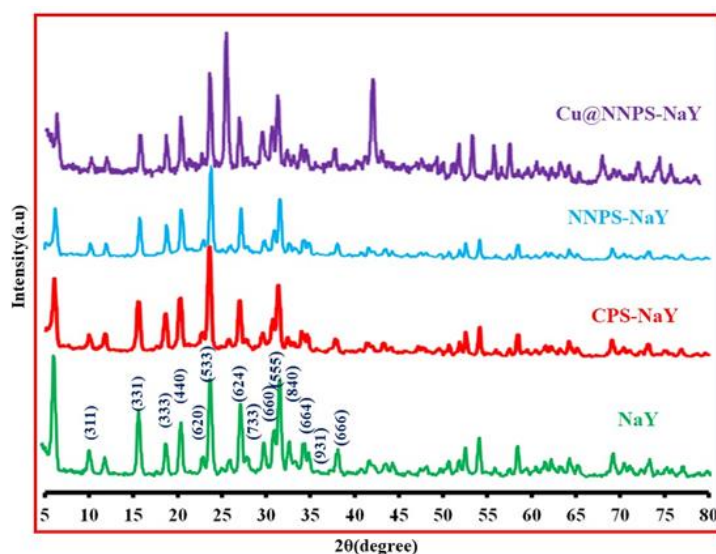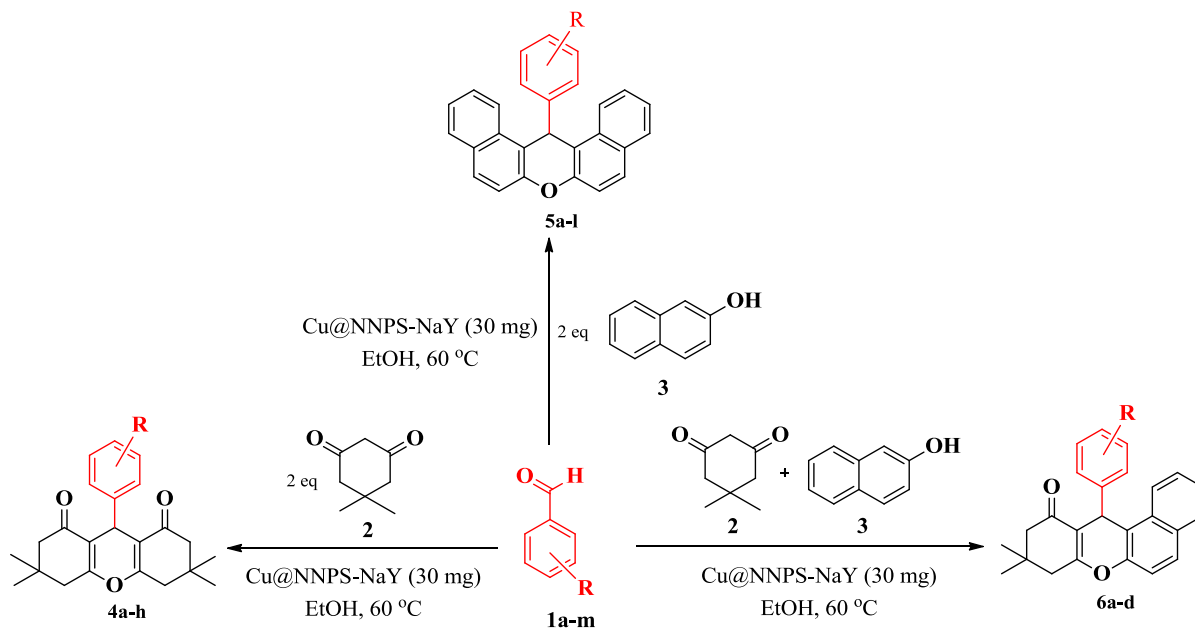


**Figure 8:** XRD patterns of the NaY, CPS-NaY, NNPS-NaY, and Cu@NNPS-NaY

**Scheme 3:** Xanthenes synthesis catalyzed by Cu@NNPS-NaY

**Table 2:** Optimization of reaction conditions for the synthesis of xanthenes

| Entry | Catalyst (mg) | Solvent | Temperature (°C) | Time (min) | Yield %[a] |
|---|---|---|---|---|---|
| 1 | NaY (10 mg) | $CH_2Cl_2$ | r.t | 120 | trace |
| 2 | CPS-NaY (10 mg) | $CH_2Cl_2$ | r.t | 120 | trace |
| 3 | NNPS-NaY (10 mg) | $CH_2Cl_2$ | r.t | 120 | 42 |
| 4 | CuI (5 mol%) | $CH_2Cl_2$ | r.t | 40 | 38 |
| 5 | NN/Cu (5 mol%) | $CH_2Cl_2$ | r.t | 40 | 70 |
| 6 | Cu@NNPS-NaY (10 mg) | $CH_2Cl_2$ | r.t | 40 | 60 |
| 7 | Cu@NNPS-NaY (10 mg) | $CH_2Cl_2$ | 40 | 40 | 66 |
| 8 | Cu@NNPS-NaY (10 mg) | $CH_2Cl_2$ | 40 | 40 | 76 |
| 9 | Cu@NNPS-NaY (10 mg) | $CH_2Cl_2$ | 40 | 40 | 78 |
| 10 | Cu@NNPS-NaY (20 mg) | $CH_2Cl_2$ | 40 | 40 | 80 |
| 11 | Cu@NNPS-NaY (25 mg) | $CH_2Cl_2$ | 40 | 40 | 83 |
| 12 | Cu@NNPS-NaY (30 mg) | $CH_2Cl_2$ | 40 | 40 | 87 |
| 13 | Cu@NNPS-NaY (35 mg) | $CH_2Cl_2$ | 40 | 40 | 88 |
| 14 | Cu@NNPS-NaY (40 mg) | $CH_2Cl_2$ | 40 | 40 | 88 |
| 15 | Cu@NNPS-NaY (30 mg) | $H_2O$ | 60 | 40 | 70 |
| 16 | Cu@NNPS-NaY (30 mg) | MeOH | 60 | 40 | 74 |
| **17** | **Cu@NNPS-NaY (30 mg)** | **EtOH** | **60** | **40** | **97** |
| 18 | Cu@NNPS-NaY (30 mg) | EtOH: $H_2O$ (2:1) | 60 | 40 | 90 |
| 19 | Cu@NNPS-NaY (30 mg) | EtOH: $H_2O$ (1:2) | 60 | 40 | 82 |
| 20 | Cu@NNPS-NaY (30 mg) | EtOH: $H_2O$ (1:1) | 60 | 40 | 86 |
| 21 | Cu@NNPS-NaY (30 mg) | $CH_3CN$ | 60 | 40 | 68 |
| 22 | Cu@NNPS-NaY (30 mg) | THF | 60 | 40 | 64 |
| 23 | Cu@NNPS-NaY (30 mg) | $Et_2O$ | 60 | 40 | 51 |
| 24 | Cu NNPS-NaY (30 mg) | *n*-Hexane | 60 | 40 | 55 |

*[a] Isolated yields.*

An investigation of the catalyst activity of the synthesized Cu@NNPS-NaY was conducted in the synthesis of xanthene derivatives through the three-component reaction between aromatic aldehydes **1**, dimedone **2,** and/or *β*-naphthol **3** (Scheme 3).

The model reaction between dimedone (2 mmol) and benzaldehyde (1 mmol) in the presence of a catalyst in dichloromethane at room temperature was used to determine the optimal reaction conditions. As shown in Table 2, only a trace of xanthene **4a** was produced in $CH_2Cl_2$ after 120 minutes in the presence of NaY and CPS-NaY (entries 1 and 2), while NNPS-NaY (entry 3) enhanced the reaction yield to 42 percent. Unsupported catalysts such as CuI and NN/Cu were tested resulting in 38% and 70% reaction yield, respectively (entries 4, and 5). In the presence of Cu@NNPS-NaY as a catalyst, the reaction yield increased to 60 % in $CH_2Cl_2$ after 40 minutes, indicating that the catalyst plays an important role in the reaction progress (entry 6). Next, we examined the effect of temperature in the presence of 10 mg of Cu@NNPS-NaY. According to the results, 60 °C was the best temperature (entry 8), and increasing the temperature did not affect product yield (entry 9). In addition, the model reaction was studied

with various catalyst amounts, and the best product yield was obtained when 30 mg of Cu@NNPS-NaY was used (entry 12). Next, the effect of solvents was investigated in the model reaction yield, indicating EtOH was the best solvent for this reaction (entry 17 compared with entries 14-16, and entries 19-24).The efficiency of the Cu@NNPS-NaY catalyst has been compared with other previously reported catalysts for synthesizing xanthene **4a** (Table 3). The model reaction with $Zr(DP)_2$ (60 mg), and $Fe^{3+}$-montmorillonite (80 mg) produced **4a** in 98, and 94 % yields in EtOH after 24 and 6 hours, and at higher temperatures, respectively (entries 1 and 2). Other catalysts, including $CaCl_2$ (entry 3), Montmorillonite K10 (entry 4), $Fe_3O_4@SiO_2$-TEA-HPA (entry 5), Nano-$WO_3$-$SO_3H$ (entry 6), PSA (entry 7), Cu (II)-Fur-APTES/GO (entry 8), and $Fe_3O_4$@THAM-Mercaptopyrimidine (entry 9) resulted in lower yields of **4a** (85-97 %) at higher temperature (entries 3-9). However, the Cu@NNPS-NaY catalyst performed the model reaction to proceed at 60 °C in EtOH to afford the product **4a** in 95 % yield after 40 minutes (entry 10), exhibiting the presented catalyst can be an excellent alternative catalyst for synthesizing xanthenes.

**Table 3:** Comparison of the catalytic synthesis of Xanthenes

| Entry | Catalyst/amount | Conditions | Time | Yield (%) [Ref] |
|---|---|---|---|---|
| 1 | Zr (DP)$_2$ [a] / (60 mg) | EtOH / reflux | 24 h | 98[35] |
| 2 | $Fe^{3+}$-montmorillonite / (80 mg) | EtOH / reflux | 6 h | 94[36] |
| 3 | $CaCl_2$ / (17 mg) | DMSO / 85-90 °C | 4 h | 85[37] |
| 4 | Montmorillonite K10 / (300 mg) | solvent-free / 100 °C | 2 h | 82[38] |
| 5 | $Fe_3O_4@SiO_2$-TEA-HPA [b] / (10 mg) | solvent-free sonication /80 °C | 1 h | 97[39] |
| 6 | Nano-$WO_3$-$SO_3H$ [c] / (19 mg) | solvent-free / 100 °C | 1.1 h | 92[40] |
| 7 | PSA [d] / (50 mg) | solvent-free / 80 °C | 50 min | 86[41] |
| 8 | Cu (II)-Fur-APTES/GO [e] / (20 mg) | $H_2O$: EtOH /50 °C | 30 min | 95[20] |
| 9 | $Fe_3O_4$@THAM-Mercaptopyrimidine [f] / (75 mg) | $H_2O$ / 80 °C | 10 min | 89[42] |
| **10** | **Cu@ NNPS-NaY [g] / (30 mg)** | **EtOH / 60 °C** | **40 min** | **95**[This work] |

[a]*Zirconium dodecylphosphonate*

[b]*Silica-coated $Fe_3O_4$ nanoparticle@silylpropyl triethylammonium heteropoly acid*

[c]*Nano-$WO_3$-supported sulfonic acid*

[d]*Phospho sulfonic acid*

[e]*Fur-imine-functionalized graphene oxide-immobilized copper oxide NPs*
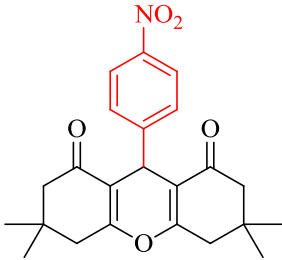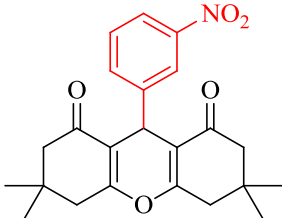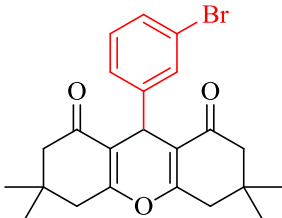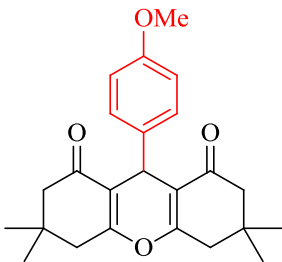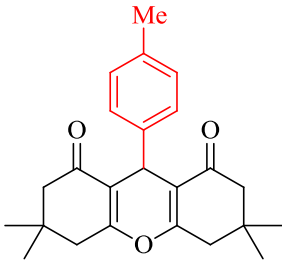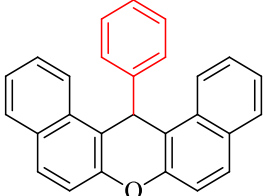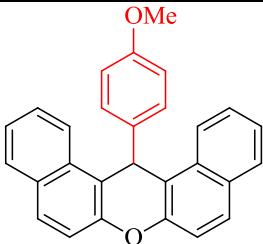
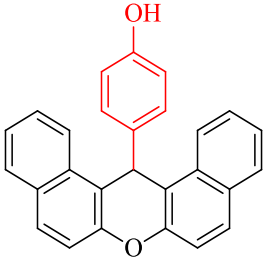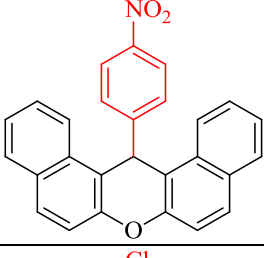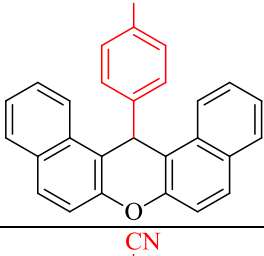[f] *$Fe_3O_4$@THAM-Mercaptopyrimidine NPs*

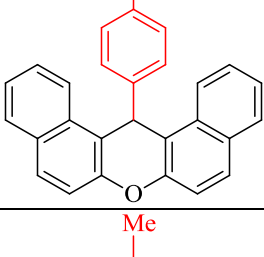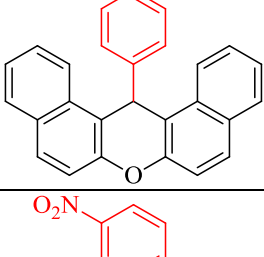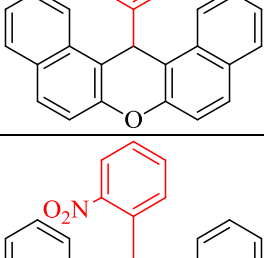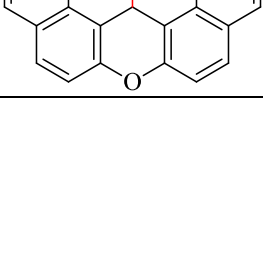[g]*copper-amine complexes on nano NaY zeolite*

As can be seen in Table 4, to extend the limitations of this method, several aromatic aldehydes **1** have been reacted under optimal conditions with dimedone **2** and/or *β*-naphthol **3**. The results showed that aldehydes with electron-donating and electron-withdrawing substituents resulted in high yields of related products. The corresponding products **4a-h**, **5a-l**, and **6a-d** were obtained in all cases with improved yields, and in shorter times than previously reported. The structure of synthesized Xanthenes has been confirmed by comparing their physical properties and $^1$H and $^{13}$C-NMR spectral data with those previously published data.
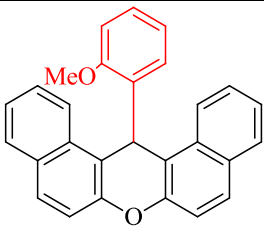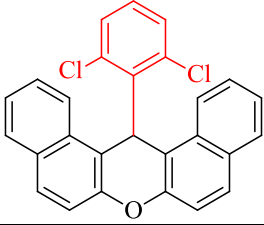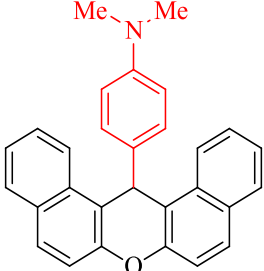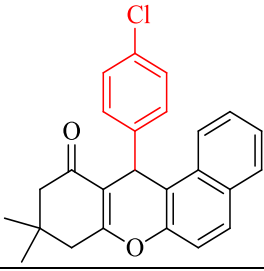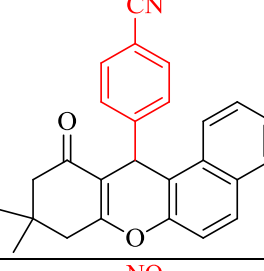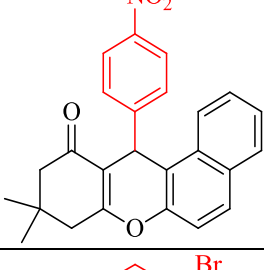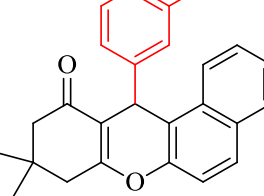
**Table 4:** Synthesis of Xanthenes using Cu@NNPS-NaY [a]



| Product | Ar | Structure | Time (min.) | Yield % [b] | Mp °C[Ref] |
|---------|-----|-----------|-------------|-------------|------------|
| **4a** | $C_6H_5$ | | 40 | 95 | 203-205[43] |
| **4b** | 4-Cl-$C_6H_4$ | | 30 | 97 | 235-237[43] |
| **4c** | 4-CN-$C_6H_4$ | | 30 | 88 | 217-219[44] |

| | | | | | |
|---|---|---|---|---|---|
| **4d** | 4-NO$_2$-C$_6$H$_4$ |  | 45 | 97 | 228-230[43] |
| **4e** | 3-NO$_2$-C$_6$H$_4$ |  | 60 | 94 | 168-170[43] |
| **4f** | 3-Br-C$_6$H$_4$ |  | 10 | 94 | 283-285[43] |
| **4g** | 4-OMe-C$_6$H$_4$ |  | 60 | 87 | 249-251[43] |
| **4h** | 4-Me-C$_6$H$_4$ |  | 30 | 90 | 232-234[45] |
| **5a** | C$_6$H$_5$ |  | 30 | 90 | 185-187[43] |
| **5b** | 4-OMe-C$_6$H$_4$ |  | 30 | 84 | 204-206[43] |

| | | | | | |
|---|---|---|---|---|---|
| **5c** | 4-OH-C₆H₄ |  | 40 | 85 | 139-141 [46] |
| **5d** | 4-NO₂-C₆H₄ |  | 40 | 95 | 316-318[43] |
| **5e** | 4-Cl-C₆H₄ |  | 60 | 96 | 282-285[43] |
| **5f** | 4-CN-C₆H₄ |  | 40 | 97 | 292-294 [47] |
| **5g** | 4-Me-C₆H₄ |  | 60 | 86 | 223-225[11] |
| **5h** | 3-NO₂-C₆H₄ |  | 10 | 87 | 216-218[43] |
| **5i** | 2-NO₂-C₆H₄ |  | 60 | 86 | 215-217[11] |

| | | | | | |
|---|---|---|---|---|---|
| **5j** | 2-Me-$C_6H_4$ |  | 30 | 82 | 262-264 [46] |
| **5k** | 2,6-diCl-$C_6H_3$ |  | 30 | 90 | 270-272 [48] |
| **5l** | 4-NMe$_2$-$C_6H_4$ |  | 30 | 94 | 289-292[49] |
| **6a** | 4-Cl-$C_6H_4$ |  | 60 | 92 | 175-178[43] |
| **6b** | 4-CN-$C_6H_4$ |  | 40 | 93 | 198-200 [50] |
| **6c** | 4-NO$_2$-$C_6H_4$ |  | 60 | 95 | 175-178[43] |
| **6d** | 3-Br-$C_6H_4$ |  | 10 | 87 | 161-164[43] |

[a]*Reaction conditions: aldehydes (1 mmol), dimedone (2 mmol) or β-naphthol (2 mmol), and 30 mg of Cu@NNPS-NaY in EtOH (10 ml), 60 °C*
[b]*Isolated yields*
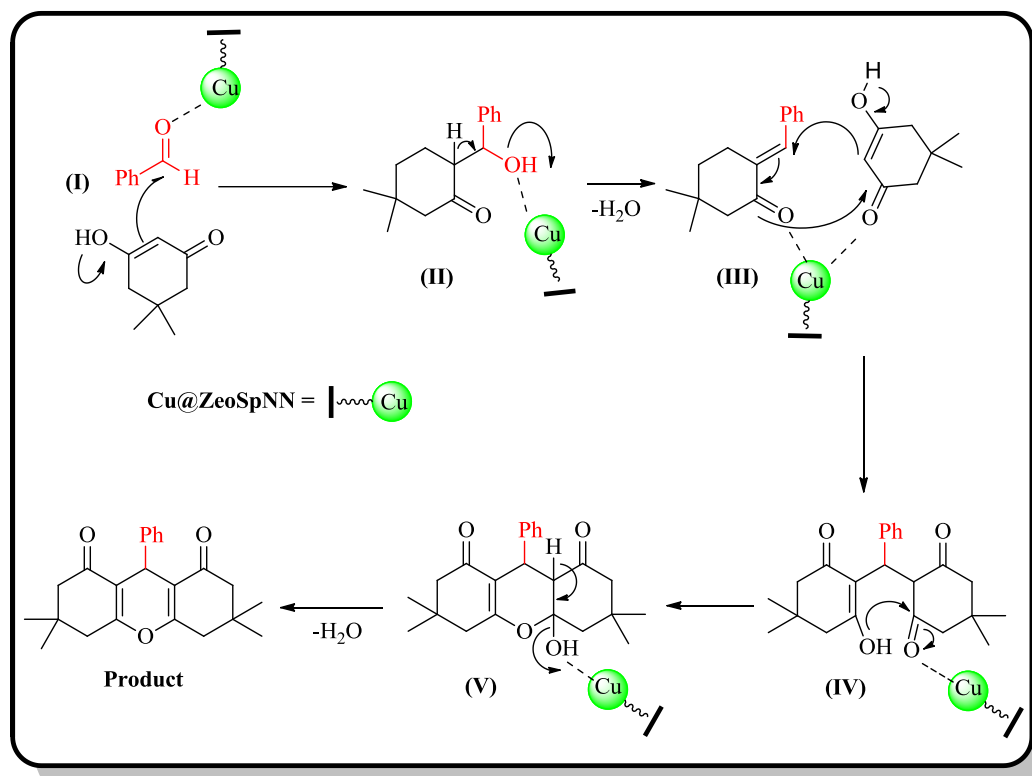
**Scheme 4:** A suggested mechanism for the Xanthenes synthesis

In the proposed mechanism, initially, the carbonyl group of aromatic aldehydes is activated by Cu@NNPS-NaY to give intermediate (I), and then dimedone attacks the activated aldehyde and affords intermediate (II). Following, removing $H_2O$ from intermediate (II), the (III) as a Michael acceptor is prepared. One more time, the Cu@NNPS-NaY activates intermediate (III). After that, Michael's addition of dimedone with intermediate (III) gives (IV). As a result of the reaction of ring closing, intermediate (IV) is converted into (V), and after removing water molecule product **4** is obtained and regenerates Cu@NNPS-NaY (Scheme 4) [11,20].

It should be noted that the synthesized catalyst is recoverable and can be reused multiple times under similar reaction conditions. Figure 9 shows that nanocatalyst Cu@NNPS-NaY displays superior catalytic performance within the twelve runs in the model reaction.
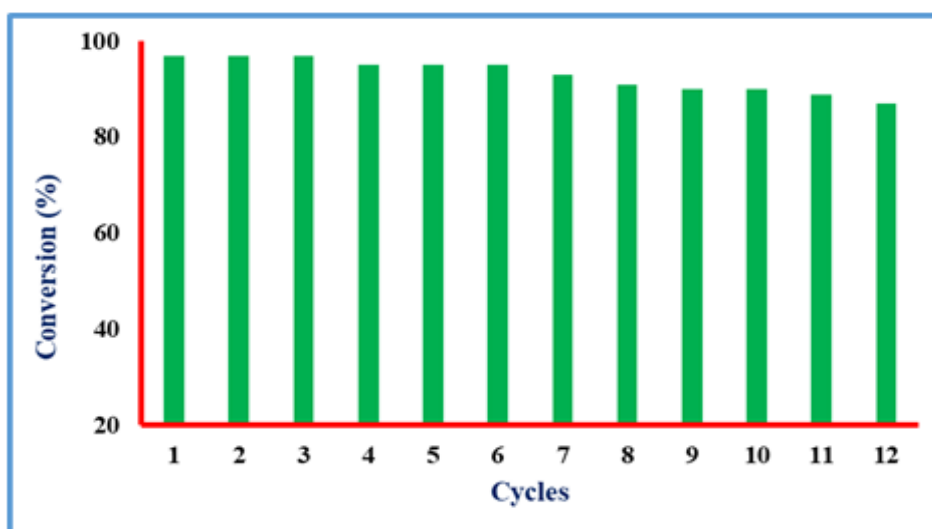


**Figure 9:** Reusability of the Cu@NNPS-NaY

Comparison of the SEM (Figure 10) and TEM (Figure 11) images of the reused Cu@NNPS-NaY after twelve successive cycles with their fresh images indicates no significant changes have been observed on the catalyst surface.

The model reaction has been tested to study catalyst leaching within the reaction process. The reaction was stopped after half-time needed for reaction completion (20 minutes) and the catalyst was removed. The product yield (81%) was determined using GC. The residue was allowed to be stirred for 20 minutes without the catalyst. The GC-analyzed reaction yield shows that there was no noticeable change in reaction yield. After 20 minutes, a copper leaching test was conducted. The ICP analysis indicated no significant difference between Cu content in the centrifuged catalyst (2.00 mmol/g) and the initial amount of copper in the NNPS-NaY (2.05 mmol/g).



**Figure 10:** SEM images of (a): fresh Cu@NNPS-NaY and (b): reused Cu@NNPS-NaY



**Figure 11:** TEM images of (a): fresh Cu@NNPS-NaY and (b): reused Cu@NNPS-NaY

## Conclusion

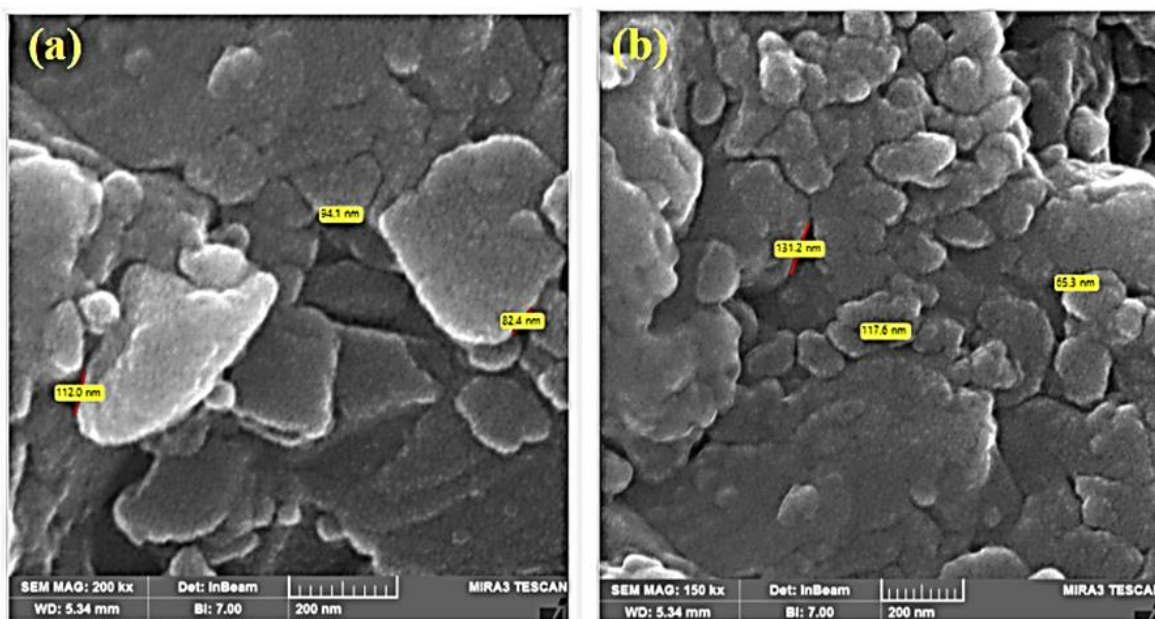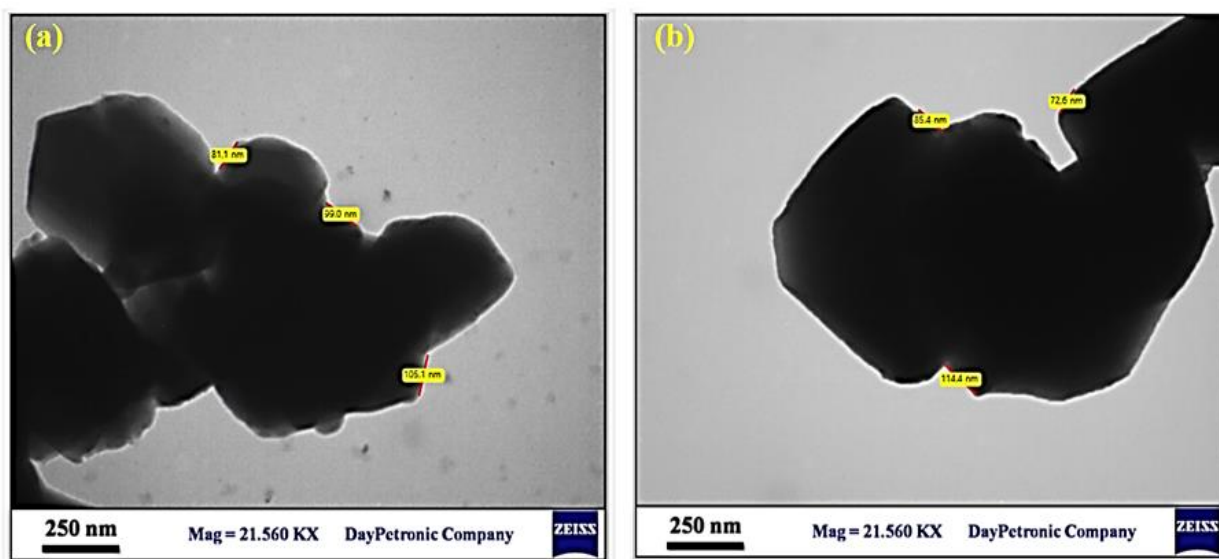The copper-amine complex Cu@NNPS-NaY was synthesized by modifying NaY nanozeolite with CPTMS, followed by treatment with 2, 2'-(propane-1, 3-diylbis (sulfanediyl)) diethanamine (NN) and coordination with Cu (I) ion. Various techniques including FT-IR, XRD, TGA, SEM, TEM, DLS, ICP, and elemental analysis were employed to determine the catalyst structure. Xanthenes are an important series of heterocycles well-known due to their outstanding pharmacological and biological properties. In this context, the activity of the synthesized catalyst was tested for xanthene derivative preparation under environmentally friendly conditions. The catalyst was filtered and reused for at least twelve consecutive runs with no significant activity loss. The catalyst's catalytic performance is improved by the presence of supported ligand NN with heteroatoms on its structure. This enhances coordination capability with copper ions and increases the homogeneity of the catalyst. The findings indicate that this catalytic system has the potential to be successful in comparable reactions. This study presents an easily replicable synthesis of beneficial heterocyclic compounds using modified NaY zeolite as a stable catalyst under mild conditions.

## Acknowledgments

## Disclosure Statement

No potential conflict of interest was reported by the authors.

## Funding

## Authors' Contributions

All authors contributed toward data analysis, drafting, and revising the paper and agreed to be responsible for all aspects of this work.

## Conflict of interest

The authors declare that there is no conflict of interest.

## ORCID

*Mohammadreza Azizi Amiri*
*https://orcid.org/0000-0001-8452-3762*
*Hamidreza Younesi*
*https://orcid.org/0000-0002-0738-7645*
*Haniye Kazemi Aqmashhadi*
*https://orcid.org/0009-0006-7606-7609*
*Ghasem Firouzzadeh Pasha*
*https://orcid.org/0000-0002-5054-2938*
*Sakineh Asghari*
*https://orcid.org/0000-0002-6608-9525*
*Mahmood Tajbakhsh*
*https://orcid.org/0000-0002-4856-1937*

## References

[1]. Centi G., Perathoner S., Catalysis and sustainable (green) chemistry, *Catalysis Today*, 2003, **77**:287 [Crossref], [Google Scholar], [Publisher]

[2]. Lam C.-w., James J.T., McCluskey R., Arepalli S., Hunter R.L., A review of carbon nanotube toxicity and assessment of potential occupational and environmental health risks, *Critical Reviews in Toxicology*, 2006, **36**:189 [Crossref], [Google Scholar], [Publisher]

[3]. Climent M.J., Corma A., Iborra S., Homogeneous and heterogeneous catalysts for multicomponent reactions, *RSC Advances*, 2012, **2**:16 [Crossref], [Google Scholar], [Publisher]

[4]. Jiang B., Rajale T., Wever W., Tu S.J., Li G., Multicomponent reactions for the synthesis of heterocycles, *Chemistry–An Asian Journal*, 2010, **5**:2318 [Crossref], [Google Scholar], [Publisher]

[5]. Maleki A., Ghassemi M., Firouzi-Haji R., Green multicomponent synthesis of four different classes of six-membered *N*-containing and *O*-containing heterocycles catalyzed by an efficient chitosan-based magnetic bionanocomposite, *Pure and Applied Chemistry*, 2018, **90**:387 [Crossref], [Google Scholar], [Publisher]

[6]. Dindarloo Inaloo I., Majnooni S., Eslahi H., Esmaeilpour M., Air-Stable $Fe_3O_4$@$SiO_2$-EDTA-Ni (0) as an Efficient Recyclable Magnetic

Nanocatalyst for Effective Suzuki-Miyaura and Heck Cross-Coupling *via* Aryl Sulfamates and Carbamates, *Applied Organometallic Chemistry*, 2020, **34**:e5662 [Crossref], [Google Scholar], [Publisher]

[7]. Montalvo S., Guerrero L., Borja R., Sánchez E., Milán Z., Cortés I., De La La Rubia M.A., Application of natural zeolites in anaerobic digestion processes: A review, *Applied Clay Science*, 2012, **58**:125 [Crossref], [Google Scholar], [Publisher]

[8]. Takmil N.F., Jaleh B., Mohazzab B.F., Khazalpour S., Rostami-Vartooni A., Nguyen T.H.C., Nguyen X.C., Varma R.S., Hydrogen production by electrochemical reaction using waste zeolite boosted with titania and Au nanoparticles, *Inorganic Chemistry Communications*, 2021, **133**:108891 [Crossref], [Google Scholar], [Publisher]

[9]. Azizi Amiri M., Pasha G.F., Tajbakhsh M., Asghari S., Copper-amine complex immobilized on nano NaY zeolite as a recyclable nanocatalyst for the environmentally friendly synthesis of 2-amino-4H-chromenes, *Applied Organometallic Chemistry*, 2022, **36**:e6886 [Crossref], [Google Scholar], [Publisher]

[10]. Younesi H., Asghari S., Pasha G.F., Tajbakhsh M., Ugi-modified nano NaY zeolite for the synthesis of new 1, 5-dihydro-2H-pyrrol-2-ones under mild conditions, *Applied Organometallic Chemistry*, 2023, e7127 [Crossref], [Google Scholar], [Publisher]

[11]. Younesi H., Asghari S., Firouzzadeh Pasha G., Tajbakhsh M., Copper-carboxamide complex immobilized on nano NaY zeolite: an efficient catalyst for xanthenes synthesis, *Research on Chemical Intermediates*, 2023, 1 [Crossref], [Google Scholar], [Publisher]

[12]. Santos S.J., Rossatto F.C., Jardim N.S., Ávila D.S., Ligabue-Braun R., Fontoura L.A., Zimmer K.R., Russowsky D., Chromene-dihydropyrimidinone and xanthene-dihydropyrimidinone hybrids: design, synthesis, and antibacterial and antibiofilm activities, *New Journal of Chemistry*, 2023, **47**:7500 [Crossref], [Google Scholar], [Publisher]

[13]. (a) Hafez H., Hegab M., Ahmed-Farag I., El-Gazzar A., A facile regioselective synthesis of novel spiro-thioxanthene and spiro-xanthene-9′, 2-[1, 3, 4] thiadiazole derivatives as potential analgesic and anti-inflammatory agents, *Bioorganic & medicinal chemistry letters*, 2008, **18**:4538 [Crossref], [Google Scholar], [Publisher] (b) Baghernejad B., Alikhani M., Nano-cerium oxide/aluminum oxide as an efficient catalyst for the synthesis of xanthene derivatives as potential antiviral and anti-inflammatory agents, *Quarterly Journal of Iranian Chemical Communication*, 2020, **8**:240 [Crossref], [Google Scholar], [Publisher]

[14]. Pinto M., Sousa M., Nascimento M., Xanthone derivatives: new insights in biological activities, *Current medicinal chemistry*, 2005, **12**:2517 [Crossref], [Google Scholar], [Publisher]

[15]. Chibale K., Visser M., van Schalkwyk D., Smith P.J., Saravanamuthu A., Fairlamb A.H., Exploring the potential of xanthene derivatives as trypanothione reductase inhibitors and chloroquine potentiating agents, *Tetrahedron*, 2003, **59**:2289 [Crossref], [Google Scholar], [Publisher]

[16]. Maia M., Resende D.I., Duraes F., Pinto M.M., Sousa E., Xanthenes in Medicinal Chemistry–Synthetic strategies and biological activities, *European journal of medicinal chemistry*, 2021, **210**:113085 [Crossref], [Google Scholar], [Publisher]

[17]. Sarma R.J., Baruah J.B., One step synthesis of dibenzoxanthenes, *Dyes and pigments*, 2005, **64**:91 [Crossref], [Google Scholar], [Publisher]

[18]. Harichandran G., Amalraj S.D., Shanmugam P., Synthesis and characterization of phosphate anchored MnO2 catalyzed solvent free synthesis of xanthene laser dyes, *Journal of Molecular Catalysis A: Chemical*, 2014, **392**:31 [Crossref], [Google Scholar], [Publisher]

[19]. Bhowmik B.B., Ganguly P., Photophysics of xanthene dyes in surfactant solution, *Spectrochimica Acta Part A: Molecular and Biomolecular Spectroscopy*, 2005, **61**:1997 [Crossref], [Google Scholar], [Publisher]

[20]. Subodh, Mogha N.K., Chaudhary K., Kumar G., Masram D.T., Fur-imine-functionalized graphene oxide-immobilized copper oxide nanoparticle catalyst for the synthesis of xanthene derivatives, *ACS Omega*, 2018, **3**:16377 [Crossref], [Google Scholar], [Publisher]

[21]. Das B., Ravikanth B., Ramu R., Laxminarayana K., Rao B.V., Iodine catalyzed simple and efficient synthesis of 14-aryl or alkyl-14-H-dibenzo [a, j] xanthenes, *Journal of Molecular Catalysis A: Chemical*, 2006, **255**:74 [Crossref], [Google Scholar], [Publisher]

[22]. El-Dafrawy S.M., Salama R.S., El-Hakam S.A., Samra S.E., Bimetal-organic frameworks (Cux-Cr100-x–MOF) as a stable and efficient catalyst for synthesis of 3, 4-dihydropyrimidin-2-one and 14-phenyl-14H-dibenzo [a, j] xanthene, *Journal of Materials Research and Technology*, 2020, **9**:1998 [Crossref], [Google Scholar], [Publisher]

[23]. Naderi S., Sandaroos R., Peiman S., Maleki B., Novel crowned cobalt (II) complex containing an ionic liquid: A green and efficient catalyst for the one-pot synthesis of chromene and xanthene derivatives starting from benzylic alcohols, *Journal of Physics and Chemistry of Solids*, 2023, 111459 [Crossref], [Google Scholar], [Publisher]

[24]. Alipour A., Naeimi H., Design, fabrication and characterization of magnetic nickel copper ferrite nanocomposites and their application as a reusable nanocatalyst for sonochemical synthesis of 14-aryl-14-*H*-dibenzo [a,j] xanthene derivatives, *Research on Chemical Intermediates*, 2023, **49**:2705 [Google Scholar], [Publisher]

[25]. Mousavifar S.M., Kefayati H., Shariati S., $Fe_3O_4$@Propylsilane@Histidine [HSO$_4$-] magnetic nanocatalysts: Synthesis, characterization and catalytic application for highly efficient synthesis of xanthene derivatives, *Applied Organometallic Chemistry*, 2018, **32**:e4242 [Crossref], [Google Scholar], [Publisher]

[26]. Zeydi M., Preparation of 1, 3, 5-Triazine-2, 4, 6-triaminium Trifluoromethanesulfonate and Its Use as an Eco-friendly Catalyst for the Synthesis of Xanthene Derivatives, *Russian Journal of Organic Chemistry*, 2022, **58**:557 [Crossref], [Google Scholar], [Publisher]

[27]. Ghamari kargar P., Bagherzade G., Beyzaei H., Arghavani S., BioMOF-Mn: an antimicrobial agent and an efficient nanocatalyst for domino one-pot preparation of xanthene derivatives, *Inorganic Chemistry*, 2022, **61**:10678 [Crossref], [Google Scholar], [Publisher]

[28]. Fallah A., Tajbakhsh M., Vahedi H., Bekhradnia A., Natural phosphate as an efficient and green catalyst for synthesis of tetraketone and xanthene derivatives, *Research on Chemical Intermediates*, 2017, **43**:29 [Crossref], [Google Scholar], [Publisher]

[29]. Zhu A., Bai S., Jin W., Liu R., Li L., Zhao Y., Wang J., An efficient and reusable ionic liquid catalyst for the synthesis of 14-aryl-14H-dibenzo [a, j] xanthenes under solvent-free conditions, *RSC Advances*, 2014, **4**:36031 [Crossref], [Google Scholar], [Publisher]

[30]. (a) Vilaça N., Amorim R., Martinho O., Reis R.M., Baltazar F., Fonseca A.M., Neves I.C., Encapsulation of α-cyano-4-hydroxycinnamic acid into a NaY zeolite, *Journal of materials science*, 2011, **46**:7511 [Crossref], [Google Scholar], [Publisher] (b) Swami M., Nagargoje G., Mathapati S., Bondge A., Jadhav A., Panchgalle S., More V., A magnetically recoverable and highly effectual Fe3O4 encapsulated MWCNTs nano-composite for synthesis of 1, 8-dioxo-octahydroxanthene derivatives, *J. Appl. Organomet. Chem.*, 2023, **3**:184 [Crossref], [Google Scholar], [Publisher] (c) Sajjadifar S., Hamidi H., Pal K., Revisiting of Boron Sulfonic Acid Applications in Organic Synthesis: Mini-Review, *Journal of Chemical Reviews*, 2019, **1**:35 [Google Scholar], [Publisher]

[31]. Asghari S., Alizadeh D., Younesi H., Firouzzadeh Pasha G., Synthesis of Spiro 1, 3-Oxazines via Three-Component Reaction of Conjugated Imines, Dialkyl Acetylenedicarboxylates and *N, N'*-Disubstituted Parabanic Acids, *Polycyclic Aromatic Compounds*, 2022, **42**:6303 [Crossref], [Google Scholar], [Publisher]

[32]. Travkina O., Agliullin M., Filippova N., Khazipova A., Danilova I., Grigor'Eva N., Narender N., Pavlov M., Kutepov B., Template-free synthesis of high degree crystallinity zeolite Y with micro–meso–macroporous structure, *RSC Advances*, 2017, **7**:32581 [Crossref], [Google Scholar], [Publisher]

[33]. Sivakumar K., Santhanam A., Natarajan M., Velauthapillai D., Rangasamy B., Seed-Free Synthesis and Characterization of Zeolite Faujasite Aluminosilicate Coating on α-Alumina Supports, *International Journal of Applied Ceramic*

*Technology*, 2016, **13**:1182 [Crossref], [Google Scholar], [Publisher]

[34]. Rongchapo W., Keawkumay C., Osakoo N., Deekamwong K., Chanlek N., Prayoonpokarach S., Wittayakun J., Comprehension of paraquat adsorption on faujasite zeolite X and Y in sodium form, *Adsorption Science & Technology*, 2018, **36**:684 [Crossref], [Google Scholar], [Publisher]

[35]. Ghassamipour S., Ghashghaei R., Zirconium dodecylphosphonate promoted synthesis of xanthene derivatives by condensation reaction of aldehydes and β-naphthol or dimedone in green media, *Monatshefte für Chemie-Chemical Monthly*, 2015, **146**:159 [Crossref], [Google Scholar], [Publisher]

[36]. Song G., Wang B., Luo H., Yang L., Fe3+-montmorillonite as a cost-effective and recyclable solid acidic catalyst for the synthesis of xanthenediones, *Catalysis Communications*, 2007, **8**:673 [Crossref], [Google Scholar], [Publisher]

[37]. Ilangovan A., Muralidharan S., Sakthivel P., Malayappasamy S., Karuppusamy S., Kaushik M., Simple and cost effective acid catalysts for efficient synthesis of 9-aryl-1, 8-dioxooctahydroxanthene, *Tetrahedron Letters*, 2013, **54**:491 [Crossref], [Google Scholar], [Publisher]

[38]. Dabiri M., Azimi S., Bazgir A., One-pot synthesis of xanthene derivatives under solvent-free conditions, *Chemical Papers*, 2008, **62**:522 [Crossref], [Google Scholar], [Publisher]

[39]. Moradi F., Abdoli-Senejani M., Silica-coated $Fe_3O_4$ nanoparticle@silylpropyl triethylammonium heteropoly acid as a nanomagnetic inorganic–organic hybrid catalyst for the green synthesis of xanthene derivatives under solvent-free conditions, *Reaction Kinetics, Mechanisms and Catalysis*, 2023, 1 [Crossref], [Google Scholar], [Publisher]

[40]. Amoozadeh A., Rahmani S., Nano-$WO_3$-supported sulfonic acid: New, efficient and high reusable heterogeneous nano catalyst, *Journal of Molecular Catalysis A: Chemical*, 2015, **396**:96 [Crossref], [Google Scholar], [Publisher]

[41]. Rezayati S., Erfani, Z.,Hajinasiri, R., Phospho sulfonic acid as efficient heterogeneous Brønsted acidic catalyst for one-pot synthesis of 14H-dibenzo [a, j] xanthenes and 1, 8-dioxo-octahydro-xanthenes, *Chemical Papers*, 2015, **69**:536 [Crossref], [Google Scholar], [Publisher]

[42]. Mir E., Hazeri N., Faroughi Niya H., Fatahpour M., Synthesis, identification and application of $Fe_3O_4$@THAM-Mercaptopyrimidine nanoparticles as a novel and highly recyclable nanocatalyst in one-pot multicomponent synthesis of 1, 8-dioxo-octahydroxanthenes and polyhydroquinolines, *Research on Chemical Intermediates*, 2023, **49**:1439 [Crossref], [Google Scholar], [Publisher]

[43]. Bhale P.S., Dongare S.B., Mule Y.B., An efficient synthesis of 1, 8-dioxooctahydroxanthenes catalysed by thiourea dioxide (TUD) in aqueous media, *Chemical Science Transactions*, 2015, **4**:246 [Google Scholar], [Publisher]

[44]. Zhou Z., Deng X., [Et3NH][HSO4] catalyzed efficient and green synthesis of 1, 8-dioxo-octahydroxanthenes, *Journal of Molecular Catalysis A: Chemical*, 2013, **367**:99 [Crossref], [Google Scholar], [Publisher]

[45]. Gong K., Fang D., Wang H.L., Zhou X.L., Liu Z.L., The one-pot synthesis of 14-alkyl-or aryl-14H-dibenzo [a, j] xanthenes catalyzed by task-specific ionic liquid, *Dyes and Pigments*, 2009, **80**:30 [Crossref], [Google Scholar], [Publisher]

[46]. Safari J., Aftabi P., Ahmadzadeh M., Sadeghi M., Zarnegar Z., Sulfonated starch nanoparticles: An effective, heterogeneous and bio-based catalyst for synthesis of 14-aryl-14-*H*-dibenzo [a, j] xanthenes, *Journal of Molecular Structure*, 2017, **1142**:33 [Crossref], [Google Scholar], [Publisher]

[47]. Kundu K.,Nayak, S.K., Camphor-10-sulfonic acid catalyzed condensation of 2-naphthol with aromatic/aliphatic aldehydes to 14-aryl/alkyl-14*H*-dibenzo [a, j] xanthenes, *Journal of the Serbian Chemical Society*, 2014, **79**:1051 [Crossref], [Google Scholar], [Publisher]

[48]. Cao Y., Yao C., Qin B., Zhang H., Solvent-free synthesis of 14-aryl-14 *H*-dibenzo [a, j] xanthenes catalyzed by recyclable and reusable iron (III) triflate, *Research on Chemical Intermediates*, 2013, **39**:3055 [Crossref], [Google Scholar], [Publisher]

[49]. Zolfigol M.A., Moosavi-Zare A.R., Arghavani-Hadi P., Zare A., Khakyzadeh V., Darvishi G., WCl 6 as an efficient, heterogeneous and reusable

catalyst for the preparation of 14-aryl-14 *H*-dibenzo [a, j] xanthenes with high TOF, *RSC advances*, 2012, **2**:3618 [Crossref], [Google Scholar], [Publisher]

[50]. Mohammadi R., Eidi E., Ghavami M., Kassaee M.Z., Chitosan synergistically enhanced by successive $Fe_3O_4$ and silver nanoparticles as a novel green catalyst in one-pot, three-component synthesis of tetrahydrobenzo [α] xanthene-11-ones, *Journal of Molecular Catalysis A: Chemical*, 2014, **393**:309 [Crossref], [Google Scholar], [Publisher]